International Journal of Engineering Inventions
e-ISSN: 2278-7461, p-ISSN: 2319-6491
Volume 13, Issue 7 [July. 2024] PP: 45-55

Study on the design of turning unit and optimization of transmission gear structure for shale gas compressor

Yong Li[a1], Debin Qiao[a], Xingbo Tang[b], Yajun Long[b], NingDan Xiong[b], Mingxing Wang[a], Jianli Wu[a], Zhen Chen[c], Nengpeng Chen[c]

(a. China Petroleum Group Jichai power Co., Ltd. Chengdu compressor branch, Chengdu, Sichuan, 610100;
b. Chongqing gas mine, Southwest Oil and Gas Field Branch of petrochina Co., LTD, Chongqing, 400707;
c. Southwest Petroleum University School of Electrical and Mechanical Engineering, Chengdu, Sichuan, 610500)

Abstract: *The turning device is the core equipment to ensure the normal operation and disassembly and maintenance of the compressor. Its transmission gear has been subjected to the instantaneous impact of the motor and the alternating load in power transmission for a long time, and the failure of the gear is inevitable. By combining theoretical calculation and numerical simulation, failure mechanism analysis of transmission gear of turning gear was carried out, and a new type of turning gear was designed and its transmission gear structure was optimized. The results showed that the theoretical calculation of transmission gear structure met the strength requirements. The maximum equivalent stress on the tooth surface is 606.54MPa, close to the allowable contact stress of the material 680MPa, and the safety factor is low, so the optimal design direction of the structure is determined. After orthogonal design, the fatigue stress of tooth root bending and contact fatigue stress of tooth surface are reduced by 31% and 36.6% respectively. The results show that the first-order natural frequency of 743.51Hz is much higher than the meshing frequency of the transmission gear 579Hz, and the resonance will not occur, which improves the reliability of the turning gear.*

Keywords: *shale gas; Compressor; Turning device; Numerical simulation; Mechanical analysis*

Date of Submission: 01-07-2024 Date of acceptance: 11-07-2024

I. Introduction

In recent years, the total consumption of natural gas in China has been increasing, and the dependence on foreign countries has reached 42.3%, resulting in the import volume of natural gas increasing year by year. The clean energy represented by shale gas is an important replacement performance source for optimizing the energy structure and energy conservation and emission reduction in China. Vigorously developing shale gas is an important means to solve the energy security in China. Shale gas compressor, as the core equipment of shale gas supercharging export, needs to be turned before and after stopping the machine. The existing turning devices mainly include manual turning and electric turning. Among them, manual turning has limitations such as time and effort, high degree of danger, difficulty in control, and dependence on operating experience. Electric turning car can not be used for high explosion-proof requirements, small working space and other occasions, and high cost, complex operation. The transmission gear of the turning gear device is subjected to complex and varied load conditions, and the working environment is harsh, which is prone to broken teeth, pitting, wear and other faults. At the same time, the reduction box is affected by the vibration frequency of the parts in the box, resulting in deformation of the box, which adversely affects the operation and installation of the internal gear transmission system. Therefore, it is necessary to carry out the structural design of compressor turning gear, the mechanical analysis of turning gear and the modal analysis of turning gear box.

At present, domestic and foreign scholars have done related research on the structure of compressor turning unit. In 2008, Wang Leqin et al. [1] summarized the design methods and steps of the conventional turning device by taking the design of the reducer turning device as an example. In 2010, Xie Libin [2] et al. changed the turning device of compressor unit from manual to electric, which met the need for continuous turning during turbine start-up and shutdown, reduced the labor intensity of employees, and facilitated the maintenance of the unit. In 2019, Fu Guohong [3] et al. installed electrical equipment on the turning device, but made its operation simple, convenient and reliable, precise stopping point and high degree of automation. In 2019, Wang Jing [4] designed a high-speed and high-torque radial meshing gear type turning gear to solve the problem of large starting

[1]Li Yong, corresponding author, engineer, Chengdu Compressor Branch of China Petroleum Group Jichai Power Co., Ltd. His main research interests is compressor manufacturing.

torque and high speed of turning gear, aiming at the need for a turning gear device to drive the feed water pump to a certain speed before the water pump small steam turbine starts to turn. In 2019, Liang Zhiwei [5] optimized the control loop of the original turning device in view of the situation that the turning device trip for no reason occurred many times during the generator shutdown and turning up. After optimization, the control system was easy to operate and the control loop was more scientific. In 2021, Sun Chao [6] et al. designed a new type of centrifugal compressor turning structure and corresponding turning tools, which can realize convenient and reusable centrifugal compressor turning alone. In 2021, Gao Chao [7] et al., aiming at the internal heating of the turning device, accelerate the air flow by increasing the wind path inside the device, so as to achieve the purpose of reducing the temperature rise. In 2023, Zhou Qin et al. [8] carried out a ratchet pawl meshing force analysis on the ratchet pawl type hydraulic turning device of steam turbine unit, and found that the maximum ratchet pawl stress near the meshing turning point reached 367MPa and 372MPa respectively, 2.6 times and 1.5 times of the optimal meshing state.

As a transmission part in the gear turning device, due to the complex and variable load conditions, the failure is more and more common, mainly tooth surface fatigue failure and tooth root bending failure, domestic and foreign scholars have carried out relevant research on this. In 2012, Ren Xingli et al. [9] simulated and analyzed the contact stress distribution of the tooth surface, and discussed the influence of the curvature of the tooth surface and the influence of the induced curvature of the tooth surface on the contact stress. In 2015, Putti Srinivasa Rao et al. [10] selected 3 different materials and combined 9 schemes for two-foot mesh, and compared the finite element analysis results with the theoretical values of Hertzian equation. In 2019, Hanoca [11] et al. studied the influence of different materials and modules on the contact stress and fatigue life of spur gears based on the finite element analysis method. In 2020, Yang Zhuxi et al. [12] proposed a contact stress calculation method for non-orthogonal modified helical gear based on the surface meshing transmission principle and Hertz contact theory, and obtained the contact stress through finite element analysis, and the error between the calculation method and the result was only 5.23%. In 2021, Liu Hui et al. [13] established the finite element model of spiral bevel gear, carried out the calculation and study of the contact stress of spiral bevel gear tooth surface containing friction, and analyzed the contact stress of gear based on different friction coefficients. In 2021, Lin Zhiji [14] carried out static analysis of cylindrical and gear contact based on the finite element analysis method, and compared it with the Hertzian contact theoretical value and the contact stress results of the tooth surface respectively to obtain the error and accuracy of the analysis results. In 2020, Subhash Chavadaki et al. [15] used two kinds of alloy materials to analyze the bending stress and deformation at different tooth root fillet radii in view of the bending fatigue failure at the tooth root. In 2022, Xue Yutong et al. [16] proposed a gear bending strength analysis algorithm based on the equal geometry method to carry out the bending strength analysis of planar gears, and compared it with the traditional gear bending stress analytical solution and the maximum bending stress at the tooth root calculated by the finite element software ANSYS. In 2023, He Zhongshi [17] et al. used simulation analysis calculation method, fourth strength theory calculation and tooth root bending fatigue theory calculation to calculate the tooth root equivalent stress of a pair of gear pairs and made a comparison.

To sum up, at present, domestic and foreign scholars mainly carry out structural design and fault analysis for the turning gear, while there are few reports on the mechanical analysis of key components of the turning gear, which is exactly the key to improve the safety and operational stability of the turning gear structure. This paper carries out structural design for the shuffling device of shale gas compressor, provides an automatic shuffling device, uses numerical simulation method to carry out mechanical analysis of the transmission gear of the shuffling device, and carries out modal analysis around the shuffling device, so as to provide guarantee for the safe, efficient and stable operation of the compressor unit.

II. Structure design of turning gear and safety analysis of transmission gear

In the process of starting and stopping of the compressor unit or during equipment maintenance, the turning gear needs to rotate forward and backward and change the speed to ensure the safe operation of the compressor unit. Under this working condition, the driving gear of the turning gear unit is under complex working condition and variable load, which can bear the instantaneous meshing force of the gear teeth for a long time. After the structural design of the turning gear unit, the safety analysis of its driving gear is conducted. The theoretical fatigue calculation of the transmission gear of the turning gear is carried out to provide a theoretical basis for the dynamic analysis of the key components of the turning gear.

2.1 Analysis of structure composition and working principle of turning device

The compressor turning device adopts horizontal arrangement, which can realize manual and automatic turning modes. It is mainly composed of reducer motor, transmission gear, worm gear reducer, box, bracket, roof, turning gear and spindle, and its overall structure is shown in Figure 1.

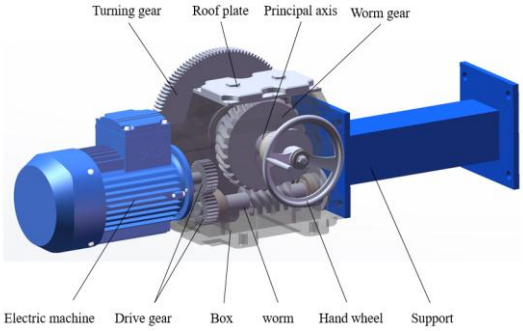

Fig.1 Overall structure diagram of shale gas compressor turning device

Compressor turning is divided into automatic and manual turning modes. In the automatic turning mode, the motor of the reducer is started, and the power is transmitted to the transmission gear. The outer meshing of the transmission gear transmits the power to the worm gear reducer. The worm wheel and the drive shaft rotate coaxial and then transmit the power to the turning gear, and drive the compressor flywheel to realize the turning gear in the form of meshing, so as to achieve the speed required by the turning gear. In the manual turning mode, the manual turning wheel transfers the power directly to the turning gear through the main shaft, and then drives the compressor flywheel to rotate and realize the manual turning. In the process of turning, the turning gear and the motor are directly connected to transmit large torque and high power, and frequently turn forward and backward, and the driving system of the turning gear device bears complex and changeable loads for a long time.

2.2 Check analysis of fatigue and stress of transmission gear of turning gear

2.2.1 Failure mode analysis of transmission gear of turning gear

The transmission gear is directly connected to the motor shaft, subject to the transient impact of the motor and the alternating load in the power transmission, the failure risk of the gear teeth is large, and the common failure forms of the turning gear mainly include fatigue pitting and tooth root breaking. In the long-term use of gear teeth, due to excessive wear, beyond the cyclic stress that the gear can withstand, in the process of power transmission, the gear teeth produce repeated bending stress, resulting in fatigue cracks on the rounded surface of the root of the tooth, and expand on the rounded surface of the root of the tooth, this repeated cyclic load causes the gear teeth to suffer bending fatigue damage. Pitting corrosion is a surface fatigue failure phenomenon of gear tooth surface cracks, because the tooth surface is subjected to alternating stress, and the contact stress exceeds the limit that the tooth surface can withstand. By optimizing the geometry of the gear, the load can be reduced and the contact stress can be reduced, thereby reducing the risk of fatigue failure.

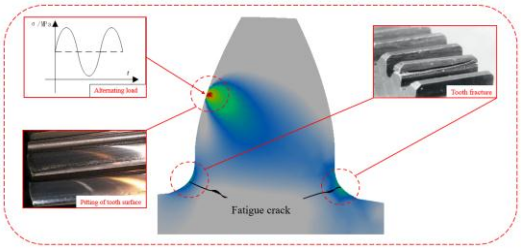

Fig.2 Gear failure form

2.2.2 Theoretical analysis of bending fatigue of transmission gear

In order to improve the fatigue failure of transmission gears, a fatigue calculation model was established for safety analysis based on the bending fatigue theory of gears. The meshing diagram of transmission gears is shown in Figure 3, and the external meshing of two gears drives parallel motor torque. The selection of materials and related parameters is shown in Table 1.

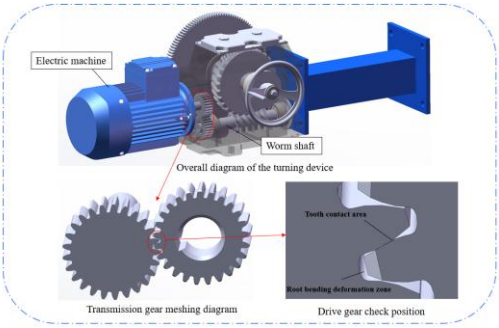

Fig.3 Transmission gear meshing position diagram

Table 1 Related parameters of transmission gear

Material	Root radius/(mm)	Number of teeth	Module	Pressure Angle/(°)	Tooth width/(mm)
20Cr	0.2	25	2	20	20

The allowable fatigue stress is obtained by taking the bending fatigue limit $[\sigma_{FE}]$ as 850mpa, and the safety factor S_F as 1.25.

$$[\sigma_{F1}] = [\sigma_{F2}] = \frac{[\sigma_{FE1}]}{S_F} = \frac{[\sigma_{FE2}]}{S_F} = 680Mpa(1)$$

When the traditional method is used to calculate the bending strength of the gear, considering the installation and processing errors, it is assumed that it is safer for the gear with general accuracy requirements to assume that all the load acts on a pair of gear teeth. In the calculation, the gear teeth are simplified into a diagonal line with a 30° Angle from the symmetrical center line of the gear teeth and a tangent to the rounded corner of the tooth root, as shown in Figure. 4. It is considered that the line between the two tangent points is the position of the dangerous section, and the tooth thickness of the dangerous section is s_F. The Angle between the normal force F_n and the vertical line of the center line of the gear tooth is α_F, the normal force F_n can be decomposed into F_1 and F_2, the bending stress of the tooth root is generated by F_1, and the component force F_2 downward of the vertical gear tooth can be ignored. Therefore, the bending stress σ_F of the dangerous section of the tooth root is:

$$\sigma_F = \frac{M}{W} = \frac{6KF_t h_F \cos\alpha_F}{bs_F^2 \cos\alpha} = \frac{KF_t}{bm} \frac{6\frac{h_F}{m}\cos\alpha_F}{\left(\frac{s_F}{m}\right)^2 \cos\alpha} \quad (2)$$

In the formula: *K* is the load coefficient; h_F is the bending lever.

By introducing the tooth shape coefficient Y_{Fa} and stress correction coefficient Y_{Sa}, the bending stress σ_F can be simplified as:

$$\sigma_F = \frac{2KT_1}{bd_1 m} \cdot Y_{Fa} \cdot Y_{Sa} \quad (3)$$

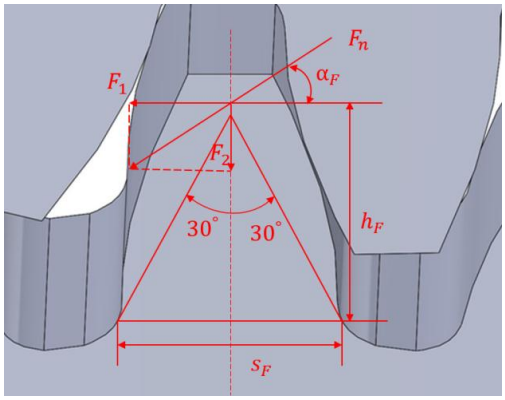

Fig. 4 Dangerous section of tooth root

Select a 5.5Kw turning motor with a speed of 960r/min to determine the motor torque:

$$T_1 = \frac{9550P}{n_1} = 54710N \cdot mm \quad (4)$$

For the torque on the worm shaft, it is driven by two gears of the same size, that is, $T_2 = T_1 = 54710N \cdot mm$, which can be obtained $\sigma_F = 341.87\text{Mpa} \leq [\sigma_F] = 680Mpa$ according to formula (3). The calculated results show that the bending fatigue strength of the tooth root meets the requirements, providing a theoretical basis for comparison with the equivalent stress calculated by subsequent simulation analysis.

III. Mechanical response analysis of transmission gear of turning gear

In order to reveal the dynamics law of turning gear during meshing, numerical simulation method was used to analyze the dynamic characteristics of turning gear, orthogonal experiment method was used to analyze and optimize the transmission gear structure considering the influence law of different root fillet radius and different materials on the maximum stress of gear, and the best design scheme was selected.

3.1 Transmission gear dynamics analysis

3.1.1 Boundary conditions and material property Settings

The material of the transmission gear is preliminarily selected as 20Cr, and the specific properties of the material are shown in Table 2.

Table 2 Specific properties of materials

Density/（kg/m^3）	Young's modulus/(Pa)	Poisson's ratio	Bulk modulus/(Pa)	Shear modulus/(Pa)
7850	2E+11	0.3	1.6667+E11	7.6923+E10

The transmission gear is set with 1/4 symmetry, and the characteristics of gear keyway, wheel hub and chamfering are ignored, and the applied torque becomes $13678N \cdot mm$. The grid division process is shown in Figure 5. The total number of grid units is 230143 and the total number of grid nodes is 332342. A rotating pair to the ground is set for the transmission gear, and the named selection surface is set as a contact pair. A frictional contact with friction coefficient of 0.15 is set, the active rotation is 3°, and $13678N \cdot mm$ hindrance torque is applied to the driven wheel. The rotation direction is the same as the direction of torque application.

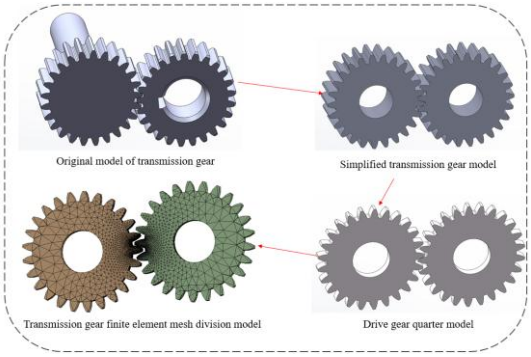

Fig.5 Finite element mesh division model

3.1.2 Stress response law analysis

The stress distribution and stress peak response law of the transmission gear of the existing turning gear are analyzed. The stress distribution is shown in Figure 6, and the maximum equivalent stress changes with time are shown in Figure 7.

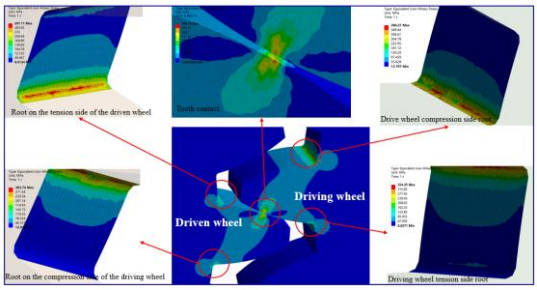

Fig.6 Stress distribution diagram of transmission gear

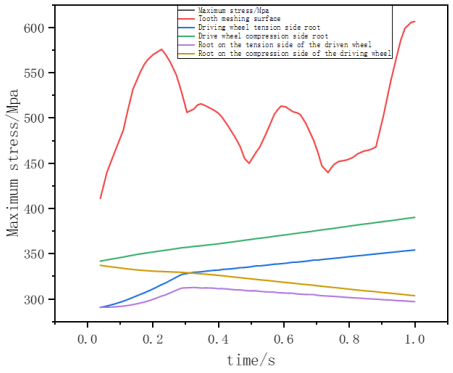

Fig.7 Maximum equivalent stress time-varying diagram of transmission gear

(1) Analysis of the overall stress distribution

The stress distribution of the transmission gear is mainly concentrated on the tooth surface and the rounded corner of the tooth root. Gear tooth surface is the main part of load transfer, and the contact stress is concentrated in the transmission gear tooth surface. The contact stress is caused by the pressure between gear tooth surfaces, and the size depends on the torque, gear geometry, gear material and other factors. When the transmission gear transmits the output torque of the motor, the root of the gear will be subjected to bending stress, resulting in a large stress concentration at the transition corner of the root of the gear, in addition, the root of the gear will also be affected by sliding shear stress between the tooth surfaces. In this paper, the stress influence law is analyzed by considering the transmission gear material and the tooth root transition fillet radius.

(2) Analysis of stress peak response law

When the turning device starts to work, the contact stress of the transmission gear surface reaches a peak value of 575.86Mpa at 0.22719 seconds after the gear teeth enter the mesh, and the maximum equivalent stress is 606.54MPa at 1 second when the gear teeth come out. This contact belongs to line contact and a large stress concentration appears.

The maximum equivalent stress at the root of the driving wheel is 390.27Mpa and appears at 1 second. The maximum equivalent stress value appears at the transition rounded corner of the pressure side of the driving wheel, the maximum equivalent stress on the tension side of the tooth root is 354.25Mpa, and the maximum equivalent stress at the root of the driving wheel is 337.33Mpa and appears at the transition rounded corner of the pressure side of the driving wheel. At this time, the instantaneous impact of the gear just entering meshing is large, and the maximum equivalent stress on the tensile side of the tooth root is 312.8Mpa.

The tooth surface contact fatigue stress is significantly higher than the bending fatigue stress at the root of the drive gear, the bending fatigue stress at the root of the drive gear is greater than that of the driven gear, and the compression side of the tooth root is significantly greater than the tension side of the tooth root, and the maximum bending stress at the rounded radius of the tooth root of the drive gear is 390.27Mpa less than the allowable stress of 680Mpa, slightly exceeding the theoretical value of 341.87Mpa.

The transmission gear of the turning gear basically meets the design requirements of the gear, but the safety factor is only 0.59 at the radius of the tooth root on the pressure side of the driving wheel, which is low, and there is still the risk of tooth root bending fatigue.

3.2 Transmission gear optimization scheme design

In order to reveal the influence of two factors on the safety performance of the gear structure, orthogonal experiments were carried out for two different materials, 20Cr and aluminum alloy, and the rounded radius of the tooth root was 0.2mm, 0.4mm and 0.6mm, respectively. The design of the test conditions was shown in Table 3.

Table 3 Simulation design of test conditions

Working condition	Root transition fillet radius/(mm)	Gear material
1（Master model）	0.2	20Cr
2	0.4	20Cr
3	0.6	20Cr
4	0.2	2024 aluminum alloy
5	0.4	2024 aluminum alloy
6	0.6	2024 aluminum alloy

(1) Comparative analysis of tooth root bending fatigue stress
As shown in Figure 8, the maximum bending stress of tooth root in all six working conditions occurs at the tooth root on the compression side of the driving wheel, and material change has little influence on the bending stress of tooth root. With the increase of tooth root rounded radius, the bending fatigue stress of tooth root decreases and the bending fatigue strength of tooth root increases. The maximum stress is 269Mpa, which is 31% lower than the original model's 390Mpa, which is far less than the allowable stress of tooth root bending fatigue 680Mpa, and the optimization of tooth root bending fatigue is more reasonable.

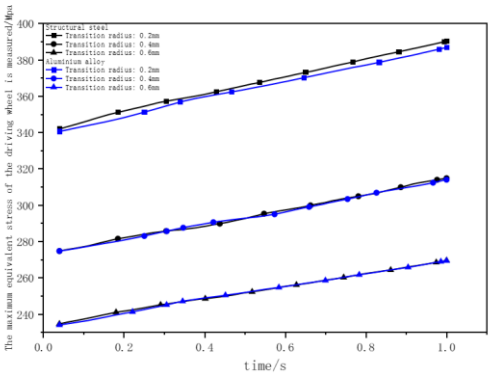

Fig.8 Influence of different root rounded radius on bending fatigue strength of tooth root

(2) Comparative analysis of tooth surface contact fatigue stress
The influence of different materials on tooth contact fatigue strength is shown in Fig. 9, when the material is structural steel, as shown in Figure. 9 (a), the original model of the tooth contact stress value is the largest, when the gear teeth into the mesh after 0.22719 seconds to reach a peak value of 659.39Mpa, when the gear material selected for the aluminum alloy, as shown in Figure. 9 (b), the maximum tooth contact stress occurs in the working condition five, when the gear teeth into the mesh after 0.32712 seconds to reach the peak value of 418.68Mpa, 36.6% lower than the original model, less than the aluminum alloy permissible contact fatigue stress, the optimization of the wheel gear performance significantly improved.

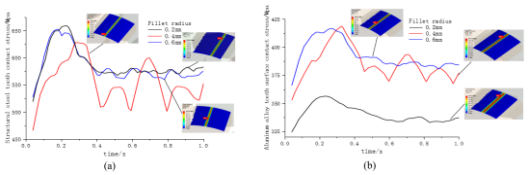

Fig.9 Influence of different materials on tooth surface contact fatigue strength

(3) Comprehensive comparative analysis of two factors
The maximum equivalent stress under six working conditions is shown in Figure 10. According to the analysis of Figure. 10, the maximum equivalent stress of working condition 6 is 353.85Mpa, which is 41.66% lower than the maximum equivalent stress of 606.54Mpa of the original model, and the bending fatigue strength of the tooth root and the contact fatigue strength of the tooth surface in working condition 6 meet the requirements. When the material is the same, the maximum equivalent stress decreases with the increase of the radius of the tooth root transition. When the radius of tooth root transition is equal, the maximum equivalent stress decreases with the increase of elastic modulus.

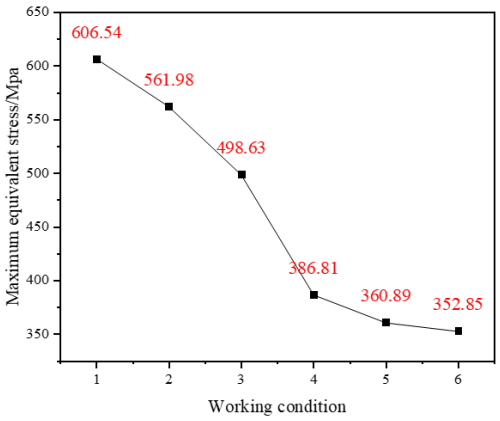

Fig.10 Results of orthogonal analysis

After optimizing the radius of tooth root and improving the selection of materials, the optimized maximum equivalent stress of the gear is reduced by 41.66%, the stress concentration of the gear is reduced, the fatigue damage of the gear is reduced, and the fracture risk of the gear teeth is reduced.

IV. Modal analysis of the box of the turning device

When the turning device is working continuously, the transmission gear is stimulated by the motor and inevitably vibrates, and is driven to the box through the shaft, which is easy to cause the box vibration, and then induce the vibration of the compressor unit, which has an adverse effect on the operation of the compressor unit. Based on the modal analysis theory, the modal analysis of the box is carried out to master its natural frequency, modal vibration and deformation, predict the vibration trend of the box, and determine whether the box resonates, so as to ensure the safety of the operation of the turning device.

4.1 Box vibration excitation analysis

The working principle diagram of the reducer box of the turning device is shown in Figure 11. The reducer motor drives an externally engaged transmission gear to transfer torque to the worm, and finally the power is staggered to the worm gear. Through analysis, the vibration source may come from the instability of the base, loose bolts, motor vibration, improper operation, etc., but the vibration excitation of the box mainly comes from the external meshing of the transmission gear driven by the motor, such vibration excitation is caused by the instantaneous impact and generally inevitable, the motor uses 0.55kw reducer motor. Its speed n1=1390r/min is the maximum input speed, and the known number of gear 1 teeth z1=25, then the transmission gear meshing frequency is:

$$f = \frac{n_1 \cdot z_1}{60} = \frac{n_2 \cdot z_2}{60} = 579Hz \qquad (5)$$

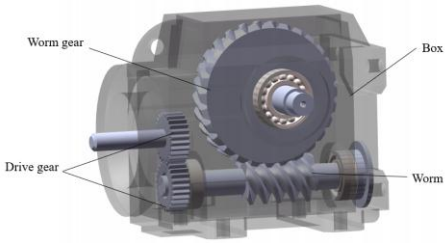

Fig.11 Working principle of the box of the turning device

4.2 Theoretical basis of modal analysis

In the calculation of the reducer box of the turning device, the natural frequency and mode mode of the box are its inherent characteristics, related to the mass distribution and stiffness distribution of the structure, the analysis of the relationship between the natural frequency and mode mode of the box is helpful to improve the box structure, so that the differential equation of the vibration of the reducer box can be established to describe its dynamic behavior.

$$[K]\{x\} + [B]\{\dot{x}\} + [M]\{\ddot{x}\} = \{F\} \qquad (6)$$

In the formula: [K], [B] and [M] are stiffness matrix, damping matrix and mass matrix; {x}, {ẋ}, {ẍ} and {F} are displacement vector, velocity vector, acceleration vector and external exciting force vector.

The modal analysis of the box is essentially to analyze the vibration characteristics of the structure itself, so the influence of the box damping and external excitation is not considered here, that is, the external excitation force

vector and damping are zero vectors, and it is simplified into an undamped vibration system. The vibration differential equation is as follows:

$$[K]\{x\} + [M]\{\ddot{x}\} = 0 \qquad (7)$$

Suppose that the structure vibrates at a certain order natural frequency, and the form of the solution is:

$$\{x\} = \{\varphi\}sin(\omega t + \varphi) \qquad (8)$$

In the formula: ω is natural frequency of the free mode of the box; φ is stands for the modal mode vector corresponding to the natural frequency.

Substituting equation (8) into equation (7), we get:

$$\{\varphi\}([K] - \omega^2[M]) = 0 \qquad (9)$$

In a physical sense, there is no point where $\{\varphi\}$ is zero, for modal analysis, each node of the box can not remain stationary, so the equation required to solve must meet:

$$det([K] - \omega^2[M]) = 0 \qquad (10)$$

Solving the natural frequency and corresponding mode of the box has been converted into solving the eigenvalue problem of the structure, but for the complex differential equation (10), it is difficult to directly obtain the analytical solution, and it needs to be solved by numerical method, among which the finite element method is a commonly used numerical calculation method.

4.3 Establishment of finite element model of box

The box model material is selected gray cast iron HT200 with relatively low price, good wear resistance and good thermal conductivity. The material properties of gray cast iron are as follows: Poisson ratio is 0.27, Young's modulus is 130Mpa, density is 7200. The mesh element size is set to 5mm, and 252261 nodes and 160212 units are obtained. The finite element model of the partited box is shown in Figure 12. The bottom surface of the box is connected to the ground bolts through the bolt holes around the box, and the bottom surface is approximately fixed constraint to realize the complete positioning of the box.

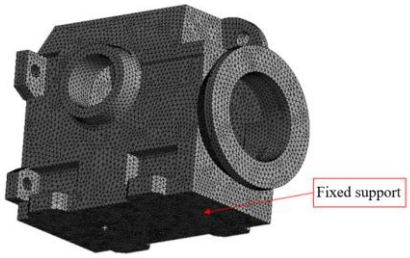

Fig.12 Boundary conditions and finite element mesh division model

The vibration mode corresponding to the low order natural frequency involves a wide range of vibration of the structure. This paper mainly analyzes the first six order natural frequency and mode mode of the box. The first six natural frequencies are shown in Table 4, and the modal shapes corresponding to the natural frequencies are shown in Figure 13.

Table 4 Description of the first six natural frequencies and vibration modes of the box

Rank	Maximum displacement/(mm)	Natural frequency/(Hz)	Mode description
Rank 1	16.601	743.51	The front end of the box vibrates along the X axis
Rank 2	19.693	1201.8	The rear end of the box vibrates torsional along the Y axis
Rank 3	14.331	1435.9	The front and rear ends of the box vibrate along the Z axis
Rank 4	23.482	1536.3	The middle end of the box vibrates along the Y axis
Rank 5	17.275	1853.5	The front and rear ends of the box vibrate torsional along the Y axis
Rank 6	29.949	2292.3	The middle end of the box vibrates along the Y axis

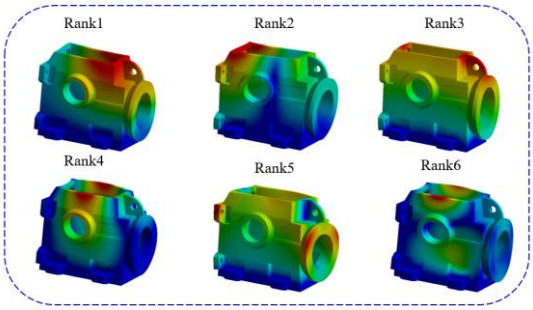

Fig.13 First six vibration modes of the box

The comparison of modal natural frequency and gear meshing frequency of the reducer box is shown in Figure 14. The natural frequency of each order of the box structure is less than the exciting frequency, which will not cause the resonance phenomenon of the reducer box.

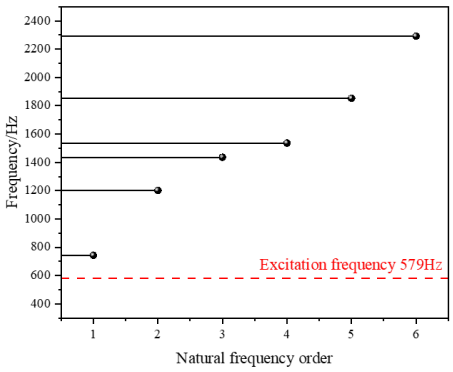

Fig. 14 Comparison between the natural frequency of the box and the meshing exciting frequency of the gear

Through the analysis of the dynamic characteristics of the transmission gear, it is shown that the transmission gear of the turning gear basically meets the safety requirements, and the meshing frequency of the transmission gear is far less than the first-order natural frequency of the box, and the box will not resonate, so the overall structure of the turning gear is safe and the turning work can be smoothly carried out.

V. Conclusion

(1) The turning gear designed in this paper is composed of the motor of the reducer, the transmission gear, the worm gear reducer, the box, the support, the roof, the turning gear and the main shaft, and has two working modes: manual and automatic. The results show that the maximum equivalent stress at the tooth surface is 606.54MPa, which is close to the allowable contact stress of the material 680MPa, and the safety factor is low, so the optimal design direction of the structure is determined.

(2) The orthogonal experimental design method was used to carry out the optimization analysis under the combination of two factors of gear material and gear transition fillet. The results showed that the optimal scheme was to determine that the tooth root transition fillet radius was 0.6mm and the material was aluminum alloy. Under this scheme, the failure resistance was good and the strength was reliable, and the maximum bending fatigue stress of the tooth root was 269Mpa. Compared with the original model 390Mpa, the peak contact fatigue stress of tooth surface is 418.68Mpa, which is 36.6% lower than the original model 659.39Mpa.

(3) The vibration characteristics of the turning gear box are analyzed, and the first six natural frequencies and modal shapes of the box are analyzed. The results show that the natural frequency increases with the increase of the order. The first natural frequency is 743.51Hz, which is much higher than the meshing frequency of the transmission gear 579Hz, and the resonance phenomenon does not occur.

References

[1]. Wang L Q, Tian Y L, Wei P, et al. Analysis and Design of Large Turning System [J]. Modern Machinery,2008,(1):1-4.

[2]. Xie G B, Wei D H. Transformation of Turning Device of Turbine Towed Air Compressor [J]. Science and Technology for Development,2010,(S1):135.

[3]. Fu G H, Qin F B, Li W J, et al. Principle and Analysis of Electric turning Gear [J]. Hydropower and New Energy,2019, volume 33 (9):44-46.

[4]. WANG J. Design of Radial Gear Gear Turning Device with High Speed and High Torque [J]. Mechanical and Electrical

Information,2019,(18): 151-152.
[5]. Liang Z W. Transformation and Application of Operation Control Technology of Large turbine generator turning gear [J]. Mechanical and Electrical Information,2019,(18): 72-73.
[6]. Sun C, Li Y J, Zhang G X. Development of turning wheel Structure and Turning Tool for centrifugal Compressor [J]. Chinese Science and Technology Journal Database (Citation Edition) Engineering Technology,2021,(9):153-155.
[7]. Gao C, Zhang Guo X, Luo X. Optimization Design of Large Synchronous Adjusting Camera Turning Device [J]. Electric Motor Technology,2021(5):27-30.
[8]. Zhou Q, Li D L. Three-dimensional finite Element Analysis of initial meshing Stress of Turbine Wheel Structure [J]. Mechanical and Electrical Equipment,2019, vol. 36 (4): 63-66, 71.
[9]. Ren X L, He G Q, Shu T L. Relationship between Tooth Surface Geometry and Contact Stress in Face Gear Transmission [J]. Journal of Hunan University of Technology,2012,(2): 49-55.
[10]. Putti Srinivasa Rao, Nadipalli Sriraj, Mohammad Farookh.Contact Stress Analysis of Spur Gear for Different Materials using ANSYS and Hertz Equation[J].International Journal of Modern Studies in Mechanical Engineering,2015,Vol.1(1).
[11]. Hanoca, P.C. Sharath, H.V. Ramakrishna.Contact Stress and Fatigue Analysis of Spur Gear[J].Applied Mechanics and Materials,2019,Vol.895: 158-163.
[12]. Yang Z X, Wu Y H, Tang J Y. Research on Contact Stress Calculation of Non-Orthogonal Modified Helical Gear Transmission [J]. Journal of Mechanical Transmission,2020, vol. 44 (2): 16-21.
[13]. Liu H, Pan W B, Ai Y S, et al. Contact Stress Analysis of Spiral Bevel Gear Tooth Surface considering Friction [J]. Science and Technology Innovation,2021,(19): 134-135.
[14]. Lin Z K, Li R G, Yan N. Three-dimensional gear contact static analysis based on finite element analysis [J]. Journal of Agricultural Engineering,2021, vol. 11 (11): 87-93.
[15]. Subhash Chavadaki, K.C. Nithin Kumar, M.N. Rajesh.Finite element analysis of spur gear to find out the optimum root radius[J].Materials Today: Proceedings,2021,Vol.46(20): 10672-10675.
[16]. Xue Y T, Zhao G, Wang A Z, He C. Geometric analysis of bending strength of spur Gear [J]. Journal of Graphics,2022, vol. 43 (1): 79-84.
[17]. He Z S, Meng L K. Comparison and calculation of equivalent stress at tooth root [J]. Marine Electric Technology,2023, vol. 43 (8): 69-73.